VI. GRAVITATION RESEARCH

Academic and Research Staff

Prof. R. Weiss
Prof. D. J. Muehlner
R. L. Benford

Graduate Students

Margaret A. Frerking
D. K. Owens

RESEARCH OBJECTIVES AND SUMMARY OF RESEARCH

Our objective is to carry out an experimental investigation of gravitational interaction which embraces terrestrial experiments and astrophysical observations. For several years the work of this group has covered a broad range. Experiments have led to the development of long-term stable gravimeters, laser strain seismometers, and molecular-beam frequency-stabilized lasers. We have also measured the fundamental phase noise in lasers and made preliminary designs of gravitational oscillators for spacecraft experiments. Astrophysical measurements have been carried out to measure the spectrum of the cosmic background radiation in the far infrared from balloon platforms, to make tests of alternative explanations of the cosmological red shift, and to study atmospheric emission in the far infrared, as well as the properties of far-infrared detectors. The inner logic or coherence of this research may not be immediately apparent. A listing of our projects demonstrates, however, that gravitational research, at least in its experimental aspects, is bound to have many facets and to spread out in various directions.

At present, we have two main areas of research. The first is infrared astronomy with primary stress on measuring cosmological observables that have a direct impact on gravitational theories. Coupled with this is the development of far-infrared technology, with emphasis on spectroscopy and the development of optical instruments and detectors. The second effort is directed toward experiments for detecting gravitational radiation from astronomical sources such as collapsing stars and ultimately the periodic radiation that may be emitted by pulsars or orbiting black holes. The experimental work involves precision optical instrumentation, digital signal processing and mechanical suspension design. Details of specific projects follow.

1. Measurement of the Isotropy of Cosmic Background Radiation in the Far Infrared

National Aeronautics and Space Administration (Grant NGR 22-009-526)

Joint Services Electronics Program (Contract DAAB07-71-C-0300)

D. J. Muehlner, R. Weiss, R. L. Benford

We have constructed and tested a balloon gondola to be used in the measurement of the large-scale isotropy of the cosmic background radiation in the spectral region 3-10 cm^{-1}. Approximately three quarters of the total energy in the spectrum is in this region. A high degree of isotropy and the thermal nature of the spectrum point to the cosmic origin of the background radiation.

One anticipated anisotropy is a first moment of the intensity distribution with angle arising from the velocity of the Earth relative to the co-moving frame that establishes a standard of rest at each point in the universe. This anisotropy can be characterized by an observation angle-dependent temperature given by

$$T(\alpha) \approx T_o\left(1 + \frac{v}{c}\cos\alpha\right),$$

where v is the velocity of the Earth relative to the co-moving frame in which the radiation is isotropic and at temperature T_o, and α is the angle between observation direction and velocity.

If the receiver spectral response extends over the entire thermal spectrum, the power received will vary with α as

$$P(\alpha) \approx P(0)\left(1 + \frac{4v}{c}\cos\alpha\right).$$

The differential radiometer that has been constructed has two horns at a zenith angle of 45° separated 180° in azimuth. For this configuration, the variation of the difference in power received by the two horns with azimuth angle ϕ is given by

$$\frac{\Delta P(\phi)}{P} = \frac{8}{\sqrt{2}}\frac{v}{c}\sin\theta_v\cos(\phi-\phi_v),$$

where θ_v and ϕ_v are the zenith and azimuth angles of the Earth's velocity vector. The maximum modulation of the power with azimuth angle occurs at the location and time at which the Earth's velocity is in the horizontal plane. The largest well-established contribution to the velocity is caused by the rotation of the Galaxy, which is $\sim 10^{-3}$ c and gives a maximum modulation in the differential power received of 0.5%.

Figure VI-1 is a schematic drawing of the apparatus. Radiation enters the instrument through two horns. At the base of the horns are mirrors that reflect into 1" light pipes that bring the radiation to a pair of interleaved reflecting choppers. The choppers alternately expose the detector to radiation from one horn and then the other. The chopping frequency is 300 Hz. Immediately below the chopper is an iris and lens-cone combination that defines the radiometer beam. The area solid-angle product of the instrument is 0.5 cm^2-steradian. The radiation is recollimated in another cone-lens combination. The function of the two back-to-back cones is to scramble the radiation from both sides of the radiometer so that the balance between the two sides of the radiometer is insensitive to misalignment of the chopper assembly and dewar which contains the detectors.

The radiation enters the liquid helium dewar through a mylar window, 0.0025 cm thick, and is guided to a capacitive grid beam splitter through a 1" stainless-steel light pipe. The beam splitter transmits low-frequency radiation and reflects high frequencies. The transmitted beam, after further filtering by another capacitive-grid low-pass filter, as well as by a piece of fluorogold, enters a lens-cone combination that matches an InSb detector to the beam.

The radiation reflected by the beam splitter contains high frequencies primarily. This beam passes through a black polyethylene filter and is collimated onto another InSb detector by another lens-cone combination.

The signal developed in either detector at the chopping frequency is proportional to the difference in power received by the two horns. Laboratory calibrations of the two channels with a thermal source give the following noise equivalent temperature differences, $\Delta T_{R.J.}/Hz^{1/2}$:

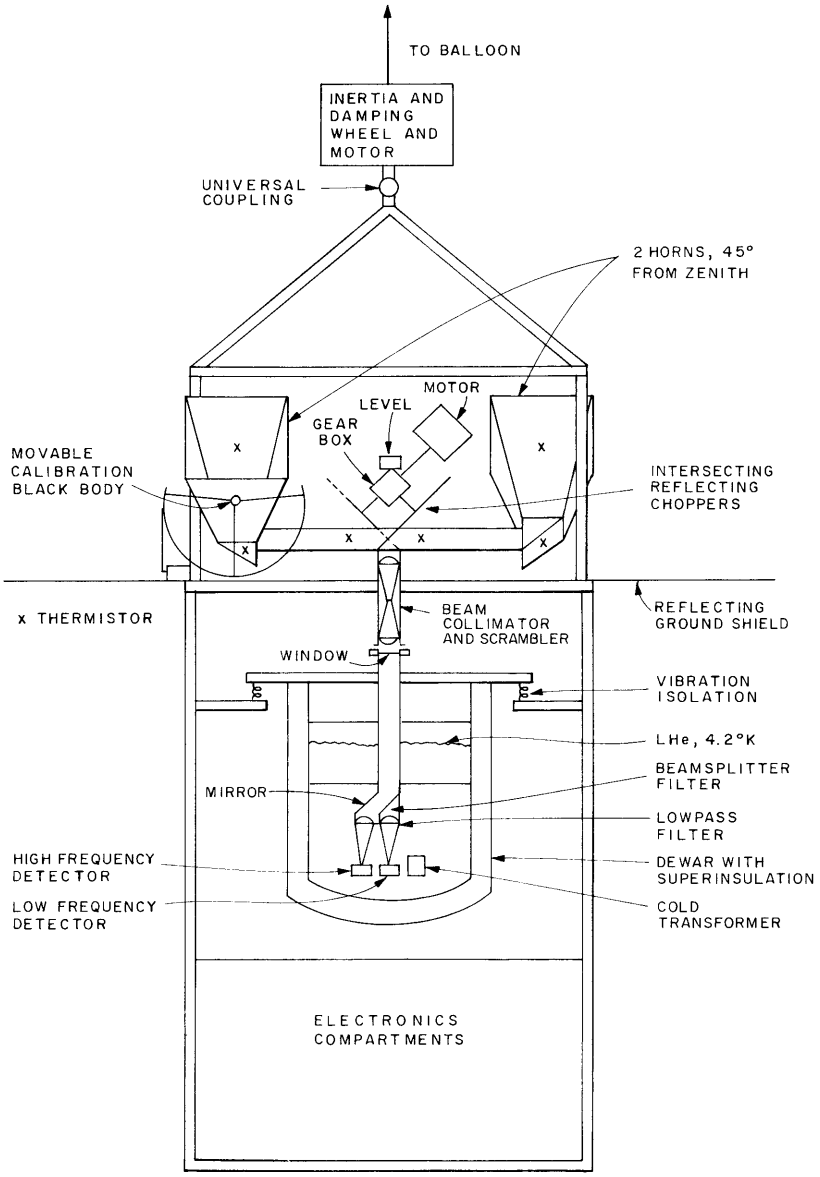

Fig. VI-1. The apparatus.

High-frequency channel	2×10^{-3} °$K_{R.J.}/Hz^{1/2}$
Low-frequency channel	1.6×10^{-2} °$K_{R.J.}/Hz^{1/2}$

If there is no additional noise from sources that will be described below, it should take 10 minutes of integration to "see" the maximum modulation caused by the Earth's motion in the low-frequency channel with a signal-to-noise ratio of 2:1.

The entire balloon gondola is supported 2000 ft below the balloon and set in rotation about the zenith at 4 rpm. The azimuthal position of the instrument is determined by measuring the Earth's magnetic field in two orthogonal magnetometers. If the background radiation is anisotropic, the odd moments of the intensity distribution will contribute a signal at the output of the radiometer at the fundamental and odd harmonics of the rotation frequency.

A small blackbody calibrator at ambient temperature that subtends $10^{-3°}$ of the beam can be placed in front of one of the horns by radio command. The horns are shielded from dust and ballast by thin mylar covers that are removed at float altitude.

Noise Sources

Signals generated by the rotation of the apparatus are indistinguishable from an anisotropy in the background radiation and may lead to systematic errors. The principal systematic noise sources that we have identified are as follows.

1. Thermal gradients induced in the warm optics by wind shear in the atmosphere.

2. Modulation of the atmospheric radiation if the horns do not maintain a constant zenith angle throughout the rotation because of the rotation-induced wobble of the gondola.

3. Density and thermal inhomogeneities in the atmosphere above the gondola which can produce both systematic errors and random noise.

4. The inevitable anisotropy by emission in the Galaxy which sets an unknown lower limit to any isotropy measurement.

There are several design features in the apparatus to reduce, or at least measure, the effect of these noise sources. The warm optical apparatus is constructed of low-emissivity materials and is sufficiently massive that the thermal time constant is much longer than the rotation period. Differential thermistor pairs are placed at symmetric points along the warm optical train to monitor temperature differences to 10^{-3} °C. At present, the emissivity of the warm optics is approximately 3%. The most critical components are the 45° mirrors under the cones because they are the farthest separated components in the optical train that are "seen" by the full beam. They contribute approximately 1% to the emissivity. With a 1% emissivity a differential temperature variation of 3×10^{-2} °C will give a signal equivalent to a 0.03% anisotropy in the background radiation in the low-frequency channel.

An instrumented bubble level that is sensitive to $10^{-3°}$ is mounted over the chopper on the rotation axis of the gondola. The rotation-induced wobble is measured with this device. In order to calibrate the variation in atmospheric signal with zenith angle in both radiometer channels, one horn and mirror can be rotated 15° in zenith angle by radio command. Using data from our previous flights to measure the background spectrum, we find that, at a zenith angle of 45°, a variation of 1/10 deg at 130,000 ft and 1/3 deg at 145,000 ft gives a signal equal to a 0.03% anisotropy of the background radiation in the low-frequency channel.

The amplitudes of the density and thermal inhomogeneities in the atmosphere above

40 km are not known. In our previous flights to measure the spectrum of the radiation, we were able to set an upper limit of 5% on the anisotropy of the radiation by the atmosphere at these altitudes. In the low-frequency channel at 40 km, the atmosphere makes a contribution equivalent to 25% of the total cosmic background radiation. In order to perform a 0.03% anisotropy measurement, the amplitude of atmospheric inhomogeneities must be less than 0.12%. Since the amplitude may be greater, our strategy is to use the signals developed in the high-frequency channel to correct the atmospheric noise in the low-frequency channel. The high-frequency channel is 30 times more sensitive to atmospheric radiation and 1/4 as sensitive to the cosmic background than the low-frequency channel.

2. Heterodyne Detection in the Far Infrared

Joint Services Electronics Program (Contract DAAB07-71-C-0300)

National Aeronautics and Space Administration (Grant NGR 22-009-526).

Margaret A. Frerking, D. J. Muehlner, R. Weiss

Tunable local oscillators for several parts of the infrared region have become available because of the steady advance of laser technology in the last few years. This development will have a profound influence on infrared astronomy, since it gives promise of narrow-band quantum noise-limited detection in the infrared. With tunable IR lasers, the heterodyne detection techniques now used in radio astronomy can be extended into the infrared. Although these detection schemes have no advantage over existing detectors for broadband measurements, they will be many orders of magnitude more sensitive than spectrometer-detector combinations in the search for spectral lines from astronomical sources in the infrared.

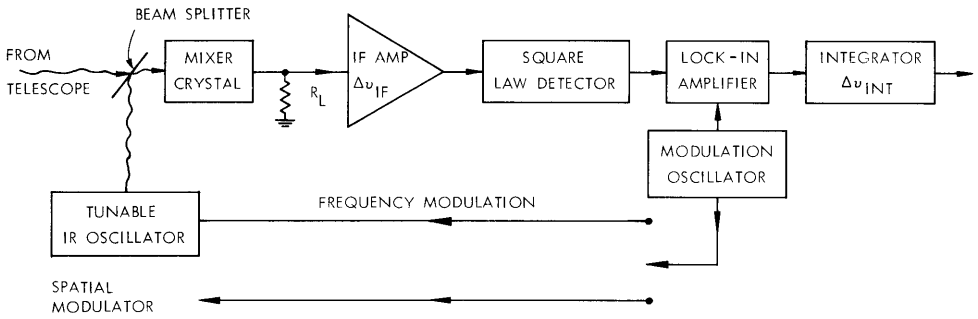

Fig. VI-2. Heterodyne detection scheme.

A typical heterodyne detection scheme is shown in Fig. VI-2. The signal from an astronomical source and the radiation from a local IR oscillator are brought together by a beam splitter and fall on a photodetector. The generated photocurrent is proportional to the square of the total incident radiation electric field. In particular, there is a component in the photocurrent at the beat frequency of the local oscillator, with the signal given by

$$i_{IF} = \frac{e\eta G}{h\nu} (2P_{LO}P_{SIG})^{1/2},$$

where i_{IF} is the photocurrent at the IF beat frequency f_{IF}, e the charge on the electron,

η the quantum efficiency of the detector, G the internal current gain of the detector, $h\nu$ the energy of the signal quantum, P_{LO} the power of the tunable IR local oscillator, and P_{SIG} the power of the incoming signal to be detected. The detector response must be fast enough that

$$\tau_{DET} \leq \frac{1}{2\pi f_{IF}}.$$

The detected signal power at the IF frequency is amplified in a low-noise amplifier with bandwidth Δf_{IF}, which is matched ideally to the bandwidth of the incoming radiation. The IF signal is envelope-detected in a square-law video detector. In order to overcome long-term gain instabilities and 1/f noise, the incoming signal may be modulated by spatial modulation in the telescope, or by periodically scanning the frequency of the local oscillator so that beat frequency between the signal and the local oscillator moves in and out of the IF bandwidth. With either type of modulation, the video output signal is synchronously demodulated and integrated in a filter with bandwidth Δf_{INT}.

The intrinsic noise sources in the detection scheme are the shot noise attributable to the photocurrent and the thermal noise of the photomixer load resistance. The IF amplifier noise can be characterized by an equivalent noise temperature which for an ideal amplifier becomes the temperature of the load resistance. The shot-noise and thermal-noise powers add:

$$P_{NOISE} = [R2eGI_T + 4kT_{eq}](\Delta f_{IF}\Delta f_{INT})^{1/2},$$

where k is Boltzmann's constant, and I_T is the total photocurrent. Generally the local oscillator dominates over all other sources so that

$$I_T = \frac{e\eta G}{h\nu} P_{LO}.$$

The condition for the minimum signal power that can be detected is

$$P_{SIG} > P_{noise}$$

$$P_{SIG} > \frac{\left[\frac{2e^2\eta G^2 P_{LO}}{h\nu} + \frac{4kT}{R_{eq}}\right](\Delta f_{IF}\Delta f_{INT})^{1/2}}{\frac{2e^2\eta^2 G^2 P_{LO}}{(h\nu)^2}}.$$

The limiting case when the local-oscillator power is large enough that local-oscillator shot noise dominates is the most interesting.

$$P_{SIG} > \frac{h\nu}{\eta}(\Delta f_{IF}\Delta f_{INT})^{1/2}$$

if

$$P_{LO} > \left(\frac{2kh\nu}{e^2 \eta G^2} \frac{T_{eq}}{R} \right).$$

In photoconductors, generation-recombination noise doubles the shot noise so that P_{SIG} is twice as large and P_{LO} is half as big. For example, at 28 μm if we use a Ge:Cu mixer with a gain of 1/3, quantum efficiency 1/2, IF and detector bandwidths of 50 MHz, and state-of-the-art amplifiers with 50 Ω input impedance, and an equivalent noise temperature of 300°K, we can detect 3×10^{-16} W with a signal-to-noise ratio of 2:1 in one second of integration. The local-oscillator power that is needed is approximately 0.4 mW.

The price paid for heterodyne detection is the small effective solid-angle area product that can be detected. The local oscillator and signal induce coherent net currents in the mixer for a beam only as large as $A\Omega = \lambda^2$. A telescope can at best only preserve this quantity.

Our first effort will be to develop heterodyne detectors at the frequencies of the rotational quadrupole transitions of molecular hydrogen and rotational electric dipole transitions of molecular hydrogen and rotational electric dipole transitions of HD in the region 10-30 μm. This region has been covered by semiconductor diode lasers composed of the lead salt $Pb_{1-x}Sn_xTe$. These lasers have been developed by the M. I. T. Lincoln Laboratory for use in molecular spectroscopy. They operate at 4°K, are electrically tunable over 0.1% of their nominal operating frequency, have a linewidth less than 1 MHz, and an output power of a few milliwatts. We will use copper-doped germanium photoconductors as mixers. A Ge:Cu crystal, 1/3 mm on a side and 2 mm long, with a donor density of $7 \times 10^{13}/cm^3$ should have quantum efficiency 1/2, detector gain 1/2, and a 60-MHz bandwidth. Part of the initial program will be to develop cryogenic IF preamplifiers with T_{eq}/R smaller than six that have a 60-MHz bandwidth. Improvements in the preamplifier reduce the output power of the laser which is required to achieve quantum noise-limited detection.

It is now believed that molecular hydrogen is a major constituent of the interior of the dark clouds in the Galaxy. In these regions molecular hydrogen can be formed by the association of hydrogen on dust grains and is shielded from dissociating ultraviolet radiation. Measurements of the column densities, kinetic temperature, and distribution among the rotational states of molecular hydrogen would add much to our knowledge of the conditions in the dark clouds. The ratio of ortho-hydrogen to para-hydrogen relates directly to the formation process on the dust grains — the question is, are the molecules only formed in the J = 0 state? The molecular chemistry and reaction rates of the heavier molecules that have been observed in these clouds in the radio region depends critically on the amount of hydrogen in the clouds. There is also some hope that by measuring the H/D ratio in the clouds by looking at the concentration of HD and H_2, we can get a new estimate of primeval D/H ratio.

Molecular hydrogen is difficult to measure spectroscopically. In optically thin regions in front of bright UV sources, molecular hydrogen can be seen in absorption by electronic transitions in the molecule. UV absorption measurements cannot be carried out in the dark clouds, and it seems that the only way to measure the molecular hydrogen concentrations directly is through the radiation by rotational transitions that occur in the far infrared.

Molecular hydrogen, which is a homonuclear molecule, has no rotational electric dipole moment and can only radiate rotational energy via quadrupole transitions with the selection rule $\Delta J = 2$. These transitions are weaker than electric dipole transitions in the ratio $(\lambda/a)^2$, where λ is the wavelength of the radiation, and a the typical

size of the molecule. At 30 μm this ratio is 10^{-9}.

HD, on the other hand, has a small electric dipole moment, $\sim 5.8 \times 10^{-4}$ debye. Although HD concentrations are expected to be 5×10^{-5} of the H_2 concentrations, the transition rates are so much faster, even for this small electric dipole moment, than the quadrupole moments of H_2 that the power radiated in HD and H_2 lines is comparable.

For the temperatures encountered in the dark clouds, 30-200°K, only the first few excited rotational levels have appreciable populations. Of the known regions, the cloud in Sgr B2 is expected to be the most powerful source of molecular hydrogen radiation. This cloud is assumed to have the following parameters: T ~ 150°K, H_2 concentration $10^6/cm^3$, D/H ~ 5×10^{-5}, distance to the cloud ~10^4 pc, and diameter of the cloud ~1.5 pc.

Table VI-1. Total power detected in the H_2 and HD lines from Sgr B2.

J → J'	$\lambda_{\mu m}$	Δf Doppler (MHz)	P_{total} watts Para-hydrogen	P_{total} watts Para-hydrogen and ortho-hydrogen	Photoconductor P_{min} coherent/Hz$^{1/2}$ (W/Hz$^{1/2}$) $\eta = 1/2$
H_2					
2 → 0	28.2	32	5.8×10^{-14}	1.7×10^{-14}	1.5×10^{-16}
3 → 1	17.03	53		2×10^{-14}	3.5×10^{-16}
4 → 2	12.28	73	1.1×10^{-15}	3.8×10^{-16}	5.6×10^{-16}
5 → 3	9.66	93		1×10^{-17}	8×10^{-16}
6 → 4	8.03	112	2.8×10^{-20}	8.3×10^{-21}	1×10^{-15}
HD					
1 → 0	112	6.7	3.3×10^{-14}		1.9×10^{-17}
2 → 1	56.2	13	4.6×10^{-14}		5.1×10^{-17}
3 → 2	37.7	20	1.1×10^{-14}		9.5×10^{-17}
4 → 3	28.5	26	8×10^{-16}		1.4×10^{-16}
5 → 4	23.1	32	1.9×10^{-17}		1.9×10^{-16}

Table VI-1 lists the anticipated total power that can be coherently detected in various H_2 and HD lines from Sgr B2. In column 1 the rotational quantum numbers of the two levels are given; in column 2 the wavelength of the transition; in column 3 the anticipated Doppler half width if the kinetic temperature is 150°K. In column 5 the minimum power that can be coherently detected in an IF bandwidth equal to the Doppler width

with a postdetection bandwidth of 1 s is given. It is assumed that the detector quantum efficiency is 1/2 and that the limiting noise is generation-recombination noise in the photoconducting mixer which is due to local-oscillator power. Noise caused by fluctuations in the background from the temperature of the mixer and its surroundings which are at 4°K is entirely negligible. Fluctuations in atmospheric emission at 300°K and emissivity 1 that fall in the IF bandwidth and are coherently detected are smaller than the local-oscillator shot noise for $\lambda < hc/kT \sim 50\ \mu m$. Column 4 has two parts for H_2 emission and one for HD. Column 4 only applies if para-hydrogen exists in the cloud, which would be the case if all H_2 molecules are formed on the dust grains in the ground state. For column 5 it is assumed that both para-hydrogen and ortho-hydrogen exist in thermal equilibrium. The power that can be detected coherently is given by

$$P = \frac{\rho_{\#} r h c \lambda}{3\pi} f(J, T)\, A,$$

where $\rho_{\#}$ is the concentration of H_2, r the radius of the cloud, λ the wavelength of the transition, f(J, T) the fraction of hydrogen in the upper rotational state J at the temperature of the cloud T, and A the Einstein spontaneous emission coefficient. It is assumed that the cloud is uniform, the lines are unsaturated, and the cloud fills the coherently detected solid-angle area product. The A coefficients for both the H_2 quadrupole transitions and the HD electric dipole transitions have been calculated by several authors.[1, 2]

Although the strongest line is expected to be the 28.2 μm line of H_2, we shall begin our measurements with the 12.28 μm line because the atmosphere is expected to absorb less than 20% at this wavelength at 4 km altitude, which is attainable from several mountain-top observatories. Furthermore, the technology of solid-state lasers is better developed at this wavelength.

The Sgr B cloud subtends a solid angle of approximately 1.5×10^{-8} ster so that at 12 μm, a telescope of 12-cm diameter will fill the solid-angle area product at the detector. If the cloud is uniform, a larger telescope will yield the same coherently detected power but with improved spatial resolution, which is significant if one wants to map the H_2 distribution and velocities within the cloud.

References

1. A. Dalgarno and E. L. Wright, Astrophys. J. 174, L49 (1972).
2. E. Bussoletti, Astron. Astrophys. 23, 125 (1973).

3. Electromagnetically Coupled Broadband Gravitational Antenna

Joint Services Electronics Program (Contract DAAB07-71-C-0300)

D. K. Owens, R. Weiss

Intensive design studies and preliminary experiments were carried out before the construction of a gravitational wave antenna of fundamentally different design from the acoustically coupled systems employed by Weber[1] and by many other groups. Our antenna design and noise calculations have been described in Quarterly Progress

Report No. 105 (pages 54-76). Briefly, the basic idea in the antenna design is the use of free masses to identify points in space. The distance between the masses, which is varied by the passage of a gravitational wave, is measured interferometrically in a multi-pass Michelson interferometer illuminated by a laser light source. There are three principal advantages of this design over acoustically coupled structures.

1. The distance between the masses (the interferometer arm lengths) can approach the wavelength of the gravitational wave. Since the sensitivity of a gravitational wave antenna is proportional to the square of its size, the ratio of the sensitivity of interferometrically coupled antennas to acoustically coupled antennas can approach the square of the ratio of the velocity of gravitational waves (assumed to be the velocity of light) to the velocity of sound in matter, which is a factor of 10^{10}.

2. Since the antenna is nonresonant and unloaded with displacement detectors, the mechanical thermal noise in the detection bandwidth can be made extremely small by using low-frequency high-Q suspensions to support the masses.

3. A broadband antenna permits direct measurement of the excitation pulse shapes for impulsive events, and facilitates optimal post-detection filtering that can be matched to the excitation spectrum.

In principle, the dominant noise in the antenna is caused by the amplitude fluctuations of the laser light intensity, and we have shown that this effect is limited by Poisson statistics. For the antenna under consideration, which uses for the interferometer arms almost confocal delay lines with mirror reflectivities of 99.5% and an argon laser light source, the minimum detectable gravitational wave strain power spectral density is approximately $10^{-32}/L^2$ Hz^{-1}. For the 10-m antenna we intend to construct, the minimum detectable strain power spectral density is expected to be

$$(\Delta\ell/\ell)^2\,(f) = 10^{-38}\ Hz^{-1}.$$

It is useful to compare this with acoustic bar antennas of the Weber type. If there are indeed astronomical sources that produce short pulses of gravitational radiation of millisecond duration, an interferometrically coupled antenna of this design would be able to detect strain pulses of $\frac{\Delta\ell}{\ell} \sim 10^{-18}$, while bars at room temperature are limited by thermal noise to 10^{-16}. In energy, this corresponds to a factor of 10^4 and would be the equivalent of the minimum detectability for a bar cooled to 10^{-2} °K.

Once such an antenna has been proved to operate as calculated it has the significant advantage that it can be increased in size. For example, a 1-km antenna would have a strain power sensitivity of 10^{-42} Hz^{-1}, which would allow a meaningful measurement of the upper limit for radiation of the Crab Nebula pulsar in one day of integration, under the assumption that 10% of the total power radiated by the pulsar goes into gravitational radiation at 60.4 Hz.

Tests carried out on a commercially available 1-W argon laser have demonstrated that the amplitude noise is within a factor of 2 of the Poisson noise limit at frequencies above 1 MHz. With a fringe phase modulation of a few megacycles produced by Pockel's cell modulators in one arm of the interferometer, it should be possible to interrogate the interferogram with Poisson noise-limited precision. The optical multi-pass delay lines have been studied both experimentally and analytically. For an almost confocal configuration characterized by a reentrant beam pattern on the mirrors, the delay line has been shown to have a second-order sensitivity in delay time to rotations of the mirrors and translations perpendicular to the main axis of the cavity. Furthermore, the angle of the output beam with the mirror nearest the beam splitter is independent of the far mirror position. The output beam appears to come out of the delay line as

though it were reflected from the near mirror.

The thorniest problem in the antenna design is that of suspensions for the masses. At present, the best, and probably most suitable, design calls for using 2-second pendulums with stiff members as part of the support fibers to drive the string modes toward high frequencies where the ground noise is small. At frequencies less than 100 Hz not all of the ground-noise isolation that is required to bring the ground noise below the equivalent laser Poisson limit can be provided by the suspension. A regression scheme that measures the ground noise on each mass as a seismometer will be required to reduce the ground noise below the Poisson noise. Our present plans are to construct a 10-m version of the antenna at the U. S. Army Ammunition Storage Depot in Natick, Massachusetts.

References

1. J. Weber, Phys. Rev. Letters 22, 1320 (1969); (1969); 25, 180 (1970).